

AlGaAs/GaAs TRANSVERSE JUNCTION STRIPE LASERS WITH DISTRIBUTED FEEDBACK

M.J. Hafich, R.A. Skogman, P.E. Petersen
Honeywell Corporate Technology Center
Bloomington, Minnesota
and
H. Kawanishi
Kogakuin University, Japan

ABSTRACT

Two AlGaAs transverse junction stripe lasers, one with distributed feedback and one with a distributed Bragg reflector, have been fabricated. Stabilized single longitudinal mode operation was obtained from both laser structures; temperature dependence of the lasing wavelength was $0.5\text{\AA}/^\circ\text{K}$ for the TJS/DBR laser and $0.63\text{\AA}/^\circ\text{K}$ for the TJS/DFB laser.

INTRODUCTION

The transverse junction stripe (TJS) laser in the AlGaAs/GaAs material system combined with a periodic feedback structure such as a distributed Bragg reflector (DBR) has the potential of being a stable, single mode optical source for GaAs integrated opto-electronics and optical communications. Periodic feedback eliminates the longitudinal mode hopping associated with conventional TJS lasers and provides control of the laser oscillation wavelength with very little device to device variation. The TJS laser configuration (see Figure 1) has both optical and electrical advantages: very low threshold currents (as low as 15mA has been reported for faceted TJS lasers¹) and single transverse mode optical fields stable over a wide range of currents and temperature.^{2,3}

TJS lasers with periodic feedback have been fabricated in two geometries (see Figure 2.)⁴. An interferometric and wet chemical etching technique was used to create a feedback grating across the entire pumping region for the distributed feedback (DFB) TJS laser and to create the separate distributed Bragg reflectors for the TJS/DBR laser. The TJS/DFB laser was a double heterostructure device grown by liquid phase epitaxy (LPE) and had a third order grating etched in the top $\text{Al}_{0.2}\text{Ga}_{0.8}\text{As}$ layer. The grating was buried by growing an $\text{Al}_{0.35}\text{Ga}_{0.65}\text{As}$ layer on the grating by metal organic chemical vapor deposition (MO-CVD). The TJS/DBR laser was also fabricated in an LPE double heterostructure. The top AlGaAs layer was thinned to $0.1\mu\text{m}$ over more than half of the laser so that the grating would be close to the GaAs active layer and optical field. Single mode operation in both configurations was obtained. The thermal shift of the laser wavelength in both cases was less than $1\text{\AA}/^\circ\text{K}$, compared to the $3\text{\AA}/^\circ\text{K}$ shift of the spontaneous emission peak.

DEVICE PROCESSING

The processing for the TJS/DFB and the TJS/DBR combines conventional AlGaAs/GaAs processing techniques with several special processes. The major steps are shown in Figure 3. For both types of lasers the gratings were in the AlGaAs layer directly above and within $0.1\mu\text{m}$ of the active layer. This avoids introducing nonradiative recombination of the injected carriers. The $\text{Al}_{0.20}\text{Ga}_{0.80}\text{As}$ layer of the TJS/DFB laser provides some optical confinement without significantly adding leakage currents around the active GaAs junction. A final layer of $\text{Al}_{0.35}\text{Ga}_{0.65}\text{As}$ was grown by MO-CVD to increase the optical field interaction for optical feedback. The GaAs homojunction was formed by a two step Zn diffusion and ohmic contacts were evaporated on both sides of the laser crystal. Individual devices were cleaved from the wafer with Fabry Perot cavity lengths on the order of $500\mu\text{m}$. The inclusion of facets for the Fabry Perot cavity simplifies testing since the structure would oscillate even at a temperature where there was not sufficient gain for the distributed feedback mode to oscillate.

EPITAXIAL GROWTH

The TJS/DBR double heterostructure was grown entirely by LPE. The three layer structure consisted of a $4\mu\text{m}$, n- $\text{Al}_{0.35}\text{Ga}_{0.65}\text{As}$ layer; a $0.4\mu\text{m}$, n-GaAs active layer; and a $7\mu\text{m}$, n- $\text{Al}_{0.35}\text{Ga}_{0.65}\text{As}$ top confining layer. The n-GaAs layer was Te-doped to a carrier concentration of approximately $2 \times 10^{18}\text{cm}^{-3}$. The structure of the TJS/DFB laser was similar except that the top confining layer of the double heterostructure was formed using a hybrid LPE/MO-CVD process. First, an undoped, $0.2\mu\text{m}$, n- $\text{Al}_{0.20}\text{Ga}_{0.80}\text{As}$ layer was grown during the LPE process. After the DFB grating was etched into this layer, an n- $\text{Al}_{0.35}\text{Ga}_{0.65}\text{As}$ layer was grown on the grating surface by the MO-CVD technique. Using MO-CVD insured the successful regrowth of AlGaAs that could not be obtained with LPE.

GRATING FABRICATION

The periodic structures for the TJS/DFB and the TJS/DBR lasers were formed by etching corrugations into the top confining layers of the double heterostructure using an interferometrically generated photoresist pattern as the etchant mask (Fig. 4). A HeCd laser ($\lambda=442\text{nm}$) was used as a light source for the interferometer. Third order gratings with periods between 350 and 400 nm were produced. Very thin photoresist, $\sim 0.1\mu\text{m}$, was used to obtain the resolution needed to form the grating. Special care was taken to align the photoresist gratings parallel to the (011) direction of the laser crystal. After a photoresist grating had been formed on the AlGaAs surface, a preferential etchant, 3:1:1 $\text{H}_2\text{SO}_4:\text{H}_2\text{O}_2:\text{H}_2\text{O}$, was used to etch the grating into the confining layer. In the TJS/DBR laser, the pumping region of the laser was protected from the grating etch by a previously applied stripe of photoresist. In both configurations, the process goal was to place the gratings as close as possible to the GaAs active layer without diminishing the gain of the active region by mechanical damage. For the TJS/DFB laser, the photoresist was cleaned after the grating fabrication and a layer of $\text{Al}_{0.35}\text{Ga}_{0.65}\text{As}$ was grown by MO-CVD on the grating surface. The next step in the TJS/DBR process was to sputter Si_3N_4 on the cleaned wafer for a Zn diffusion mask.

ZINC DIFFUSION

The Zn diffusion that forms the p⁺-p region of the TJS laser diode was performed in a semi-open ampoule in a two step process. 170nm of low oxygen content silicon nitride was sputtered over the entire wafer and a window for Zn diffusion was opened by Freon plasma etching. The initial p⁺ diffusion was made at 700°C in a flowing H₂ atmosphere with a ZnAs₂ source. Diffusion times up to two hours were required to have the p⁺ region penetrate to a point just above the GaAs active layer. To form the p-region, the sample was annealed at 900°C in flowing hydrogen with the epilayers lying face down against the quartz boat to minimize material loss.

Figure 5 is a scanning electron microphotograph showing the Zn diffusion profile through the double heterostructure. Because the energy bandgap of the lightly doped n-GaAs region was slightly wider than that of the heavily doped p-GaAs active region, the low doped n-GaAs layer in the grating region of the TJS/DBR laser acts as a low loss optical passive waveguide for laser light emitted in the heavily doped p-region.

The final step of the fabrication process was to make ohmic contacts to the n and p regions of the lasers. Evaporated AuGe and Cr/AuZn were used as the n and p ohmic contacts. Both contacts were annealed simultaneously at 460°C. Each wafer was cleaved into separate devices with lengths of 300 to 600 μm. For heat sinking during testing, the lasers were mounted with In solder p-side down on the Au plated copper heat sinks.

RESULTS

A scanning electron micrograph of a finished TJS/DBR laser without ohmic contacts is shown in Figure 6. Figure 7 shows the lasing spectra of a TJS/DBR laser for heat sink temperatures from 133°K to 153°K. In this sample, approximately 9% Al was included in the active layer making the lasing wavelength shorter than that for GaAs. The laser was pumped by applying current pulses with a duration of 200ns and repetition rate of 3Kbits. The laser had a 140μm pumping region with a 220μm long distributed Bragg reflector on one end and a cleaved facet on the other end of the cavity (See Figure 6). Lasing output was measured at the cleaved facet. At 133°K, the wavelength for the DBR mode was longer than the peak wavelength of the spontaneous emission (a few f.p.modes appear) by about 28Å, and the intensity of this mode was not maximum because mismatching occurred between the DBR mode and the spontaneous peak. At 147°K, the matching was obtained and the intensity of the DBR mode increased substantially. The threshold current was 1.3 A at 147°K. Mismatch between the two wavelengths began to appear again as the heat sink temperature was further increased, and the DBR mode wavelength became shorter than that of the spontaneous peak at 153°K. In this temperature range, the DBR mode shifts continuously from 8008Å without longitudinal mode hopping.

The pulsed lasing spectra of a TJS/DFB laser (cavity length of 550μm) for heat sink temperatures varying from 289°K to 307°K is shown in Figure 8. The experimental procedure was similar to that used for the TJS/DBR laser. The thermal behavior of the DFB mode was very similar to that of the DBR mode. The DFB mode was coincidental with the peak of the spontaneous emission at 299°K. The DFB mode oscillated at room temperatures because of an accurate calculation of the equivalent refractive index of the active waveguide, and the grating period.

Figure 9 shows the light output vs. injection current (I-L) characteristics as a function of the heat sink temperature for the TJS/DFB laser. At 289°K, where there was a large mismatch between the DFB-mode and the spontaneous emission peak, the I-L

characteristic was soft due to the relatively large amount of spontaneous emission. As the temperature was increased to 299°K, the intensity of the spontaneous emission decreased and a much sharper I-L characteristic was obtained. At 307°K, the I-L curve was similar to that of 299°K; however the light output began to saturate with the increase of injection current due to the heating of the active region. This data shows that the differential quantum efficiency was nearly independent of the heat sink temperature.

Temperature changes have two effects on the optical output of TJS/DFB and TJS/DBR lasers. First, the peak of the spontaneous emission shifts with temperature causing the amplitude of the DBR or DFB mode to vary as was shown in the data of Figures 7 and 8. The shift in the spontaneous emission peak was measured to be 3Å/°K which was in close agreement with the shift of the energy gap in GaAs. Secondly, the DFB and DBR modes shift with temperature. The DBR thermal mode shift was measured to be 0.5Å/°K, and the DFB thermal mode shift was measured to be 0.63Å/°K. The stability of the modes of the periodic feedback lasers depends largely on the laser waveguide's refractive index variation with temperature. Calculations of the difference in the waveguide effective refractive index at different temperatures were in close agreement with the experimental data, assuming an index change of $4 \times 10^{-4}/^{\circ}\text{C}$ in a simple slab waveguide produces a thermal temperature mode shift of 1Å/°C. Because of the dependence of the refractive index the thermal shifting of the DFB or DBR modes cannot be totally eliminated; however, unlike the mode hopping of the Fabry Perot cavity, the DFB or DBR mode shift was small and continuous.

CONCLUSION

Two new laser structures have been fabricated: an AlGaAs/GaAs TJS/DFB laser and an AlGaAs/GaAs TJS/DBR laser. Both devices operated in a single longitudinal mode; maximum power was obtained at 147°K (threshold current 1.3Å) from the TJS/DBR and at 298°K (threshold current 0.78Å) for the TJS/DFB laser. No mode hopping was observed for the temperature ranges used. The temperature dependence of the lasing wavelengths was 0.5Å/°K and 0.6Å/°K for the TJS/DBR and the TJS/DFB lasers, respectively.

REFERENCES

1. S. Nita, H. Namizaki, S. Takamiya, and W. Susaki, "Single-mode junction-up TJS lasers with estimated lifetime of 10^6 hours", IEEE J. Quantum Electron, vol. QE-15, pp. 1208-1209, Nov. 1979.
2. H. Kumabe, T. Tanaka, H. Namizaki, M. Ishii, and W. Susaki, "High temperature single-mode CW operation with a junction-up TJS laser:", Appl. Phys. Lett. 33, No. 1, pp. 38-39, July 1978.
3. H. Namizaki, Trans. IECE Japan, Vol. E-59, pp. 8-15, 1975.
4. H. Kawanishi, M. Hafich, B. Lenz and P. Petersen, "AlGaAs Transverse Junction Stripe Laser with Distributed Bragg Reflector", Electronics Letters, Vol. 16, No. 19, pp. 738-740, 1980.

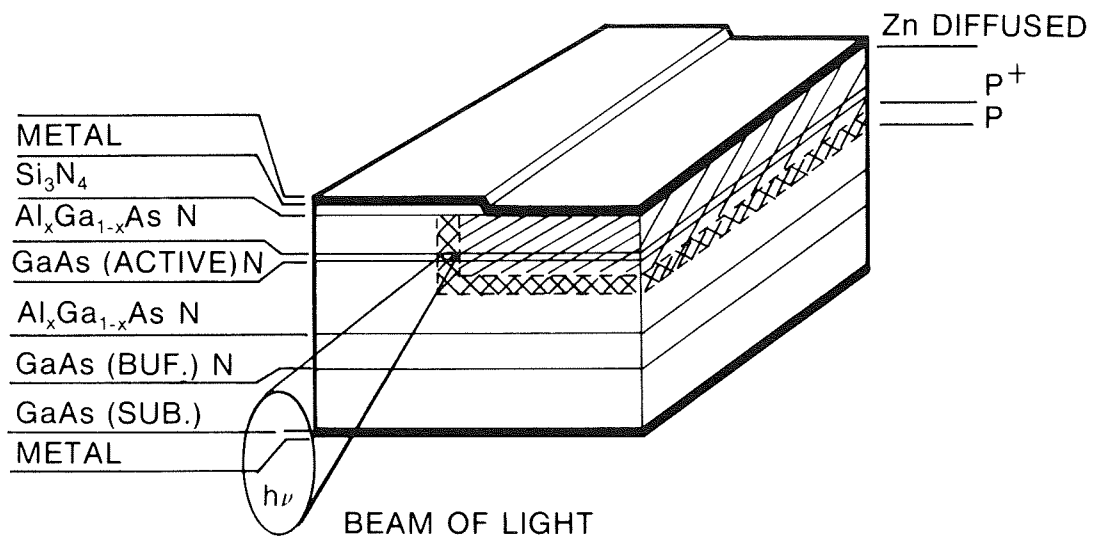


Figure 1.- Schematic of a TJS laser.

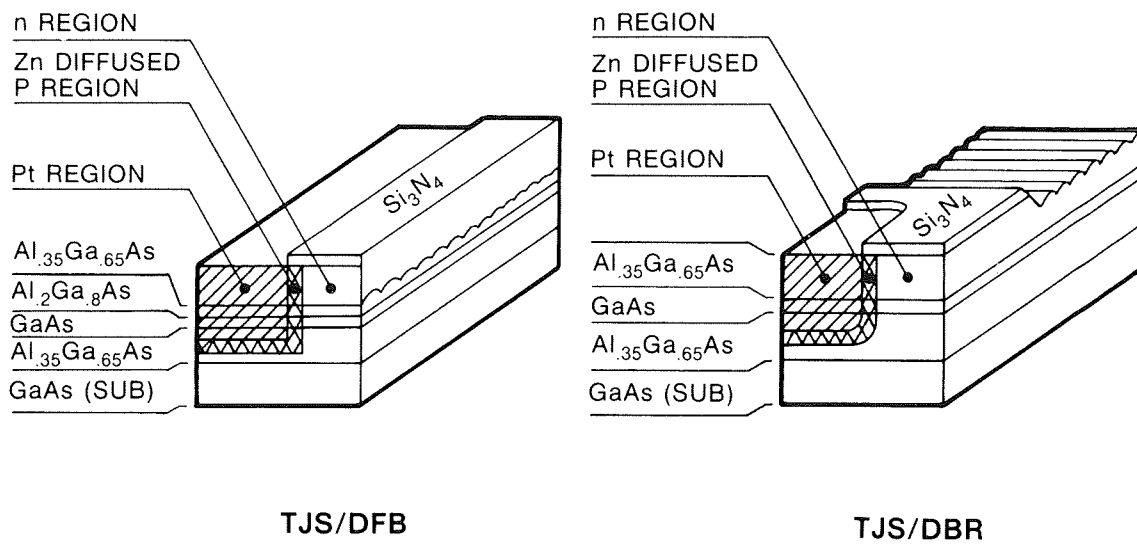
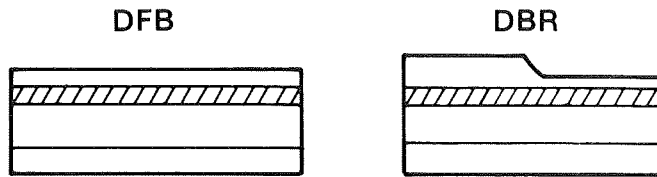
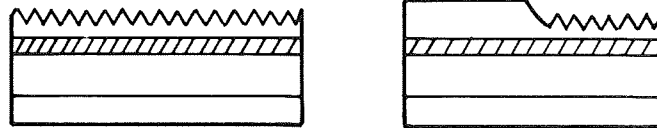


Figure 2.- Structure of the TJS/DFB and TJS/DBR laser diodes.

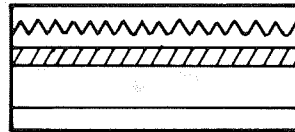
GROW EPILAYERS BY LPE
THIN DBR TOP AlGaAs TO
WITHIN 0.1 TO 0.2 μ M OF
ACTIVE LAYER.



USE INTERFEROMETRY AND
WET CHEMICAL ETCH TO
FABRICATE GRATING.



GROW DFB TOP AlGaAs LAYER
ON GRATING BY MO-CVD.



FORM P⁺-P REGIONS WITH
ZN DIFFUSION. EVAPORATE
METAL OHMIC CONTACTS.
CLEAVE OUTPUT FACETS.

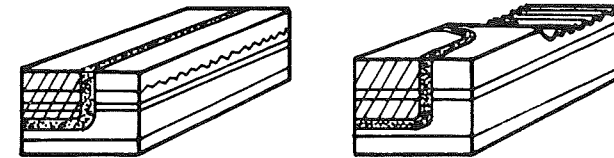
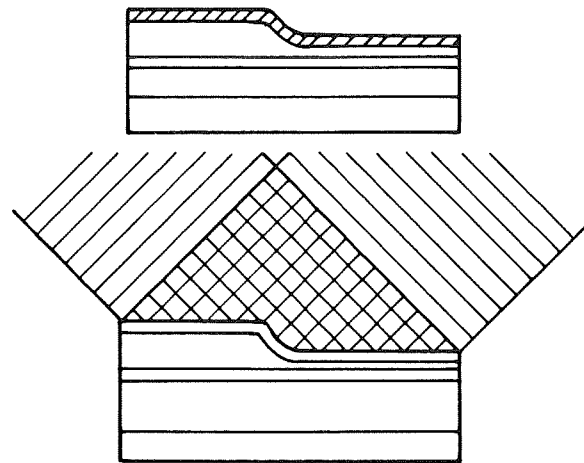


Figure 3.- Major processing steps for TJS/DFB and TJS/DBR laser diodes.

SPIN COAT LASER WAFER
WITH $\sim 0.1\mu$ M OF PHOTORESIST
1:1, AZ1350B: AZ THINNER



EXPOSE RESIST IN HeCd
INTERFEROMETER, $\lambda = 442$ NM, FOR
THIRD ORDER GRATING PERIODS
OF 350NM TO 400NM

ETCH GRATING INTO AlGaAs
LAYER ALONG (01 $\bar{1}$) PLANES. USE
3:1:1, H₂SO₄:H₂O₂:H₂O ETCHANT.

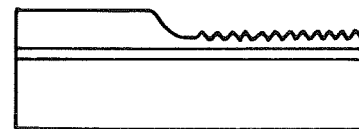


Figure 4.- Grating fabrication process.

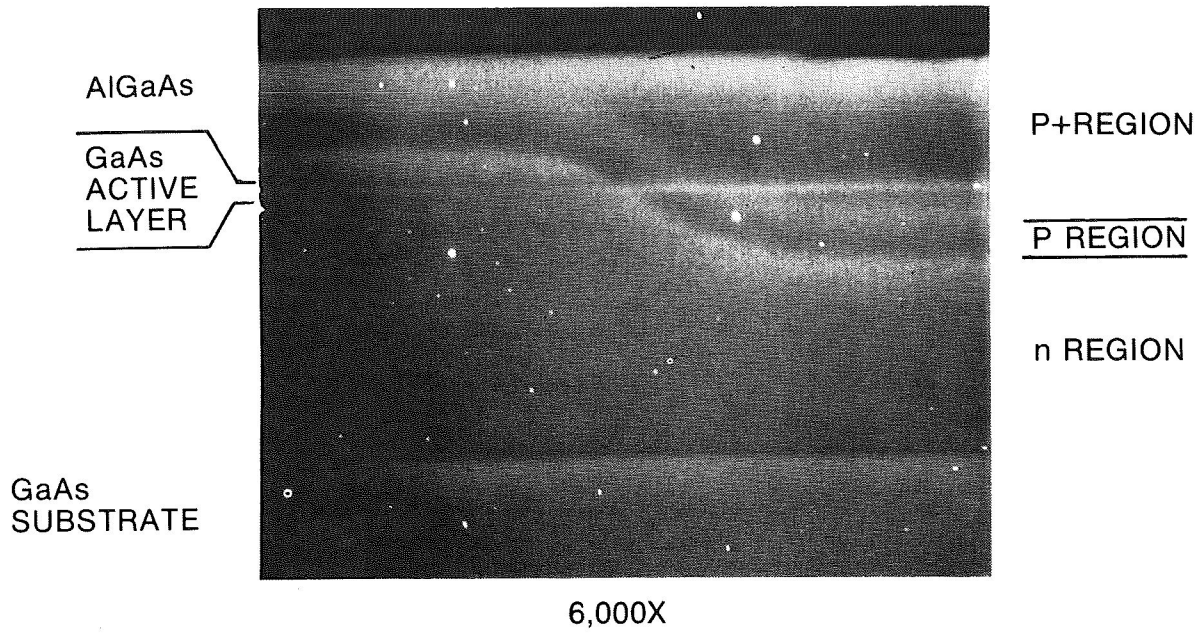


Figure 5.- Scanning electron micrograph of the Zn diffusion in an AlGaAs/GaAs double heterostructure.

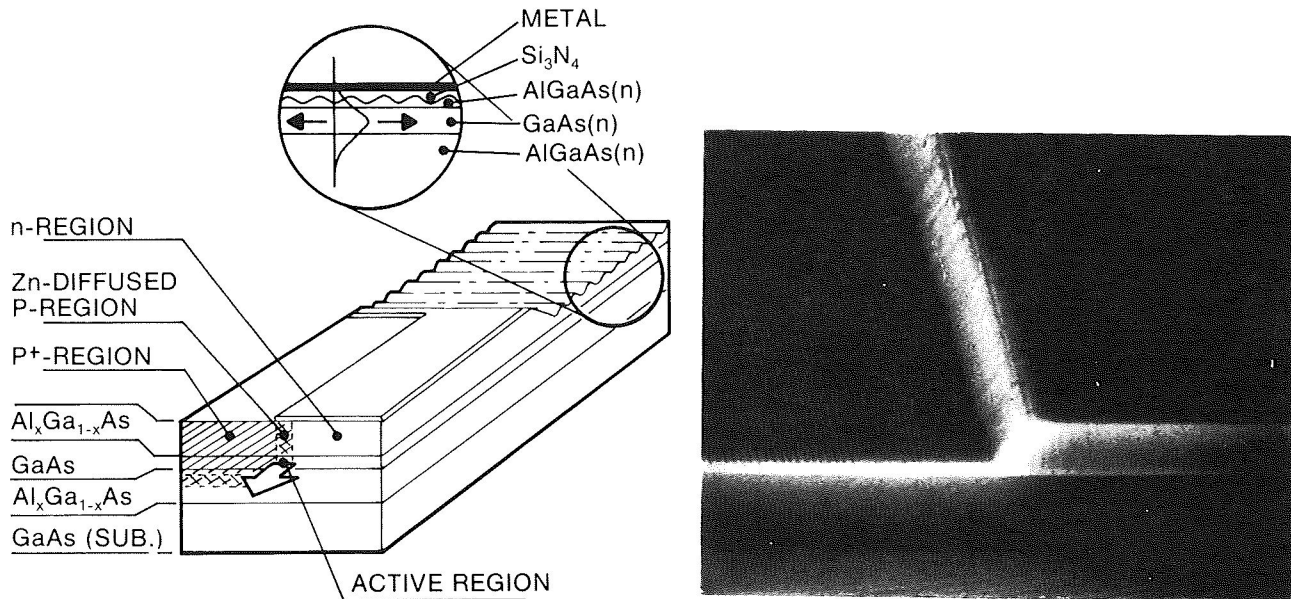


Figure 6.- Scanning electron micrograph and schematic of the completed TJS/DBR laser.

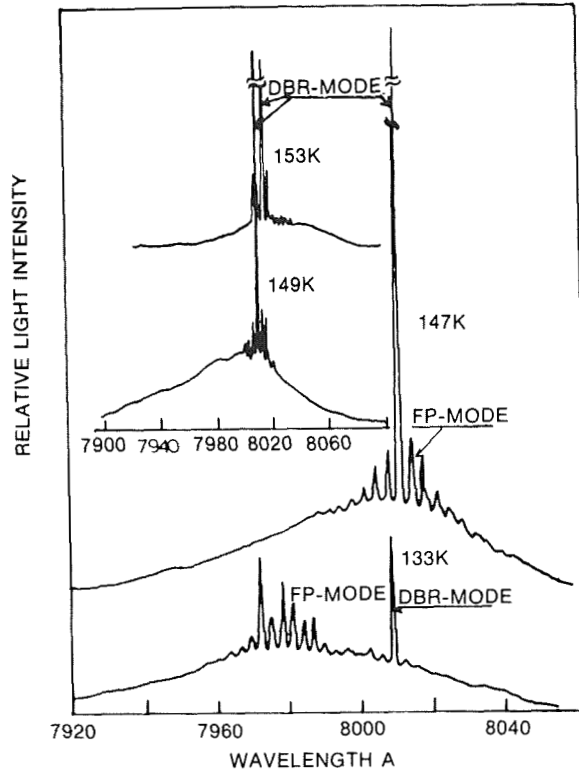


Figure 7.- Mode spectra of the AlGaAs/GaAs TJS/DBR laser between 133°K and 157°K.

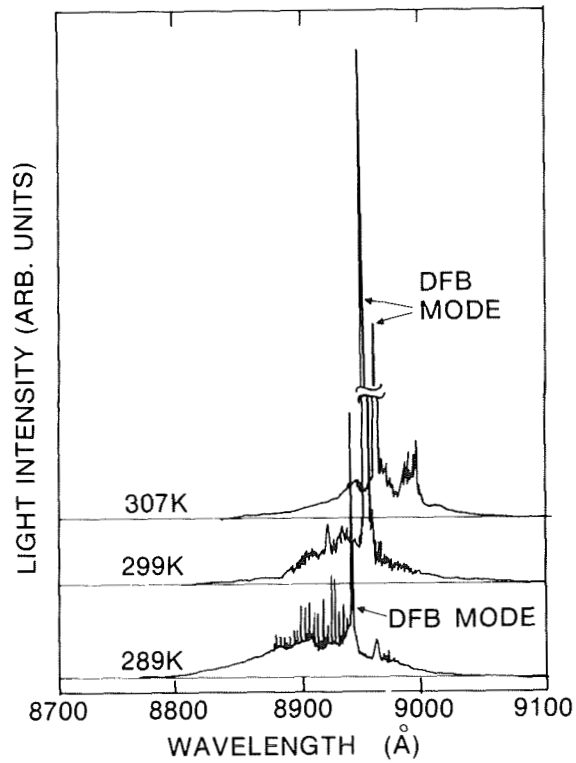


Figure 8.- Mode spectra of the AlGaAs/GaAs TJS/DFB laser near room temperature.

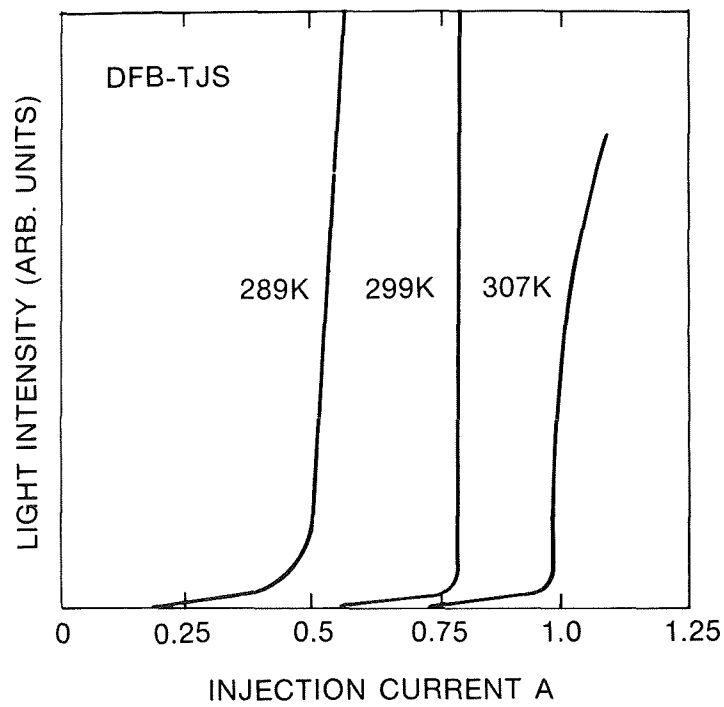


Figure 9.- Light output as a function of injection current (I-L) characteristics of the TJS/DFB laser.